Synchronization of noisy systems by stochastic signals

Alexander Neiman,[1] Lutz Schimansky-Geier,[1,2] Frank Moss,[1] Boris Shulgin,[3] and James J. Collins[3]
[1]*Center for Neurodynamics, University of Missouri at St. Louis, St. Louis, Missouri 63121*
[2]*Institute of Physics, Humboldt University at Berlin, Invalidenstrasse 110, D-10115 Berlin, Germany*
[3]*Center for BioDynamics and Department of Biomedical Engineering, Boston University, 44 Cummington Street, Boston, Massachusetts 02215*
(Received 8 December 1998; revised manscript received 5 April 1999)

We study, in terms of synchronization, the *nonlinear response* of noisy bistable systems to a stochastic external signal, represented by Markovian dichotomic noise. We propose a general kinetic model which allows us to conduct a full analytical study of the nonlinear response, including the calculation of cross-correlation measures, the mean switching frequency, and synchronization regions. Theoretical results are compared with numerical simulations of a noisy overdamped bistable oscillator. We show that dichotomic noise can instantaneously synchronize the switching process of the system. We also show that synchronization is most pronounced at an optimal noise level—this effect connects this phenomenon with aperiodic stochastic resonance. Similar synchronization effects are observed for a stochastic neuron model stimulated by a stochastic spike train. [S1063-651X(99)11407-7]

PACS number(s): 05.40.−a

I. INTRODUCTION

Recently, the phenomenon of synchronization [1,2] has been generalized to two new important classes of systems—chaotic systems and stochastic systems. Full synchronization of chaos [3,4] and phase synchronization of chaotic systems [5] have been studied, and the concept of generalized synchronization of chaotic systems was proposed in Refs. [6,7]. Synchronizationlike phenomena have also been observed in purely stochastic systems, where the noise controls a characteristic time scale of the system. Both the phenomenon of mutual synchronization of stochastic bistable systems [8] and forced synchronization (by external periodic signals) [9,10] have been demonstrated in stochastic systems with a noise-controlled time scale. Thus, the classical concept of phase synchronization has been applied to the last-named case of forced synchronization [11]. In particular, it has been shown that noise-induced switching between metastable states of a system can be *instantaneously* synchronized by an external periodic force.

In previous studies, the synchronization of stochastic bistable systems was considered for periodic driving signals or deterministically chaotic driving forces [12]. However, for many practical applications, stochastic driving signals are relevant [13]. Such signals are especially relevant to biological systems, such as ion channels [14,15] and sensory neurons [16], where signals are typically stochastic in nature or contaminated by noise.

Here we show that *noisy systems* which do not have any deterministic natural frequency can be synchronized by a *stochastic driving signal*. We study this new type of synchronization in a simple but generic kinetic model, which represents a wide class of stochastic bistable systems. Basically, we consider a bistable system with thermal noise, perturbed by an external dichotomic stochastic signal. In this system, we assume that the magnitude of the external signal is insufficient to cause a transition in the noise-free system.

The paper is organized as follows. In Sec. II, the generic kinetic model is introduced. Section III is devoted to an analytical study of the model, including the calculation of cross-correlation measures, the mean switching frequency, and synchronization regions. In Sec. IV, analytical results are compared with numerical results for an overdamped stochastic bistable oscillator driven by dichotomic noise. In Sec. IV, the instantaneous phase is introduced and the effect of phase synchronization is demonstrated. Numerical simulations of a stochastic neuron model are presented in Sec. V. Finally, the results are summarized and discussed in Sec. VI.

II. SIMPLIFIED FOUR-STATE MARKOVIAN MODEL

In most studies of stochastic resonance [17–20], the stochastic bistable dynamics is modulated by an external *periodic* signal, so that the periodic force represents an external ''clock'' [19] which is able to synchronize stochastic switching events instantaneously [11,20]. In the present study, we aim to show that a similar synchronization effect can be obtained for a stochastic signal, represented by a dichotomic Markovian process. Thus, in the situation we consider, the system is driven by two noises: the first is broadband Gaussian noise which represents internal (or thermal) noise, while the second, a dichotomic noise, represents an input stochastic signal. Although such a signal is random, it possesses a characteristic time scale, represented by the inverse flipping rate between its two states. This then leads us to consider whether the external dichotomic noise can synchronize the switching dynamics of the system. Thus, we understand synchronization in a classical way of instantaneous matching of switching events at the input and output.

The response of a bistable system to a weak stochastic input can be studied in the framework of linear response theory (LRT) [21]. This approach will be used for calculations of the cross-correlation measures. However, synchronization effects of phase and frequency locking lie beyond the limits of LRT. An analytical treatment of bistable systems driven by dichotomic noise is possible with a simplified model that captures the main features of the physical situation. A two-state model for studying fluctuating symmetrical bistable systems was first used by Debye [22], and applied in Refs. [23,24] for the purpose of calculating mean escape rates in systems with fluctuating barriers [25]. Moreover, a simplified two-state model with periodic modulation was used in Ref. [26] to study stochastic resonance.

Assume that the stochastic bistable system possesses two symmetric metastable states $\sigma(t)=\pm 1$ and is characterized by the mean switching rate a_0. We assume that the switching rate depends on the internal noise intensity D according to the Arrhenius law

$$a_0(D)=\alpha_0 \exp\left(-\frac{\Delta U}{D}\right), \tag{1}$$

where α_0 is a prefactor and ΔU represents the barrier height. Suppose now that dichotomic noise influences the bistable dynamics as an additive input signal. As a result, the Kramers rate [Eq. (1)] changes. If $d(t)=\pm 1$ corresponds to the values of the input dichotomic stochastic signal, we suppose that the rates vary according to the relations

$$\begin{aligned} W_{-1\to+1}(d(t)) &= a_0(D)\exp\left[\frac{Q}{D}d(t)\right], \\ W_{+1\to-1}(d(t)) &= a_0(D)\exp\left[-\frac{Q}{D}d(t)\right], \end{aligned} \tag{2}$$

where Q is the magnitude of the input signal. The input signal $d(t)$ switches between two states ± 1 with flipping rate γ, so that its correlation function is

$$R_{dd}(\tau)=\exp(-2\gamma\tau). \tag{3}$$

We neglect completely intrawell fluctuations (see also Ref. [26]). However, as we will show below, our simplified model exhibits good agreement with a detailed numerical simulation of a flow stochastic bistable system.

The magnitude of the input signal is always smaller than the barrier height: $Q<\Delta U$. This restriction guarantees that the signal itself cannot switch the system from one state to another. However, below we will consider input signals that are sufficiently large so as to lead to situations where the new rates of the system,

$$a_1=\alpha_0 \exp\left(-\frac{\Delta U+Q}{D}\right), \quad a_2=\alpha_0 \exp\left(-\frac{\Delta U-Q}{D}\right), \tag{4}$$

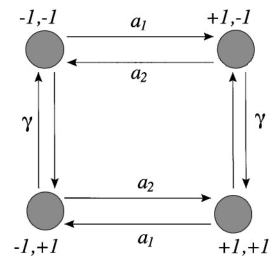

FIG. 1. Schematic of the model. The first index marking states of the system refers to the output σ, while the second index refers to the state of the input dichotomic noise d; γ is the flipping rate of the input signal and $a_{1,2}$ are the modified rates [Eq. (4)] of the system.

allow the consideration of the following rate separations: (i) $a_1 \ll a_2 \ll \gamma$, (ii) $a_1 \ll \gamma \ll a_2$, and (iii) $\gamma \ll a_1 \ll a_2$. We point out that for a fixed $\gamma \ll \alpha_0$, all three cases can be subsequently approached by changing the noise intensity D only. The latter condition also guarantees the adiabatic limit of the rates a_1 and a_2 [27].

The two states of the output $\sigma(t)$ and the two states of the input $d(t)$ form a four-state Markovian system, which is shown schematically in Fig. 1. In Fig. 1, the states of the system $\{\sigma,d\}$ are marked by the two indices, referring to the output and input, respectively. The dynamics of the system is described by the master equation for the conditional probability density $P_{\sigma,d}=P(\sigma,d,t|\sigma_0,d_0,t_0)$:

$$\begin{aligned} \partial_t P_{\sigma,d} &= -(W_{\sigma\to-\sigma}(d)+\gamma)P_{\sigma,d}+\gamma P_{\sigma,-d} \\ &\quad + W_{-\sigma\to\sigma}(d)P_{-\sigma,d} \end{aligned} \tag{5}$$

with stationary solutions

$$\begin{aligned} P^S_{-1,-1} &= P^S_{+1,+1}=\frac{a_2+\gamma}{2(a_1+a_2+\gamma)}, \\ P^S_{-1,+1} &= P^S_{+1,-1}=\frac{a_1+\gamma}{2(a_1+a_2+\gamma)}. \end{aligned} \tag{6}$$

The master equation allows a full time-dependent analysis, including calculation of auto correlation and cross-correlation functions. From the regression theorem, every ensemble-averaged statistical quantity $M(t)$ is governed by a linear differential equation which, in our case, takes the following form:

$$\begin{aligned} &\frac{d^3M(t)}{dt^3}-2(a_1+a_2+2\gamma)\frac{d^2M(t)}{dt^2}+[(a_1+a_2)^2+2\gamma(3(a_1+a_2)+2\gamma)]\frac{dM(t)}{dt} \\ &\quad -2(a_1+a_2)\gamma(a_1+a_2+2\gamma)(M(t)-M^S)=0. \end{aligned} \tag{7}$$

This can be solved for given initial conditions $d^2M/dt^2(t=0)$, $dM/dt(t=0)$, $M(t=0)$, and $M^S=M(t\to\infty)$. With the eigenvalues

$$\lambda_1=2\gamma,\quad \lambda_2=a_1+a_2,\quad \lambda_3=a_1+a_2+2\gamma, \tag{8}$$

the solution of Eq. (7) in the form

$$M(t)=A_1e^{-\lambda_1 t}+A_2e^{-\lambda_2 t}+A_3e^{-\lambda_3 t}+M^S \tag{9}$$

reduces the problem to finding the constant coefficients (A_1,A_2,A_3) from the initial conditions.

III. MEASURES OF STOCHASTIC SYNCHRONIZATION

A. Cross-correlation based measures

Linear measures of synchronization are based on the cross-correlation functions between the output process $\sigma(t)$ and the input stochastic signal $d(t)$. The simplest measure is the stationary correlation coefficient ρ:

$$\rho=\frac{\langle\sigma d\rangle}{\sqrt{\langle\sigma^2\rangle\langle d^2\rangle}}. \tag{10}$$

In the case of an extremely weak signal, $Q\to 0$, all cross-correlation measures can be obtained in terms of LRT. This theory has been successfully applied to stochastic resonance and related phenomena [21,28–30]. According to LRT, all cross-correlation quantities can be expressed through the susceptibility of the system, $\chi(\omega)$. In particular, if $G_{dd}(\omega)$ is the spectral density of the signal, then the cross-spectral density $G_{d\sigma}(\omega)$ is $\chi(\omega)G_{dd}(\omega)$ [30]. For a two-state symmetric system, the susceptibility is given by [22,29]

$$\chi(\omega)=\frac{1}{D}\frac{a_0}{a_0-\mathrm{i}\omega}, \tag{11}$$

which leads to a simple formula for the correlation coefficient:

$$\rho_{LRT}=\frac{a_0Q}{D(\gamma+a_0)},\quad Q\to 0. \tag{12}$$

According to LRT, the correlation coefficient possesses a single maximum as a function of noise intensity D [30].

For our purposes (i.e., to synchronize stochastic switching dynamics), the magnitude of dichotomic noise could be rather large. This situation is beyond the limits of LRT. On the other hand, the master equation approach allows one to obtain the *exact* expressions for the correlation functions in the framework of the simplified model.

Using the stationary solutions of the master equation (6), the correlation coefficient is

$$\rho=\frac{a_2-a_1}{a_1+a_2+2\gamma}. \tag{13}$$

In the limit $Q\to 0$, we indeed recover the LRT result [Eq. (12)]. The correlation coefficient is shown in Fig. 2 as a function of noise intensity D for different values of signal magnitude Q and flipping rate γ. First, we see that the degree of input–output correlation is maximal at a certain noise intensity, which recalls aperiodic stochastic resonance [13]. With an increase in Q, the correlation coefficient indeed increases. Note that for a large enough signal magnitude ($Q=0.2$), the dependence $\rho(D)$ flattens, and the correlation coefficient takes its maximal value in a certain region of noise intensity. We will see further that this behavior reflects mean switching frequency locking, which is a sychronization effect that cannot be revealed in the framework of LRT. With an increase in flipping rate, the correlation coefficient decreases, reflecting the low-frequency response property of bistable systems [28,31,21].

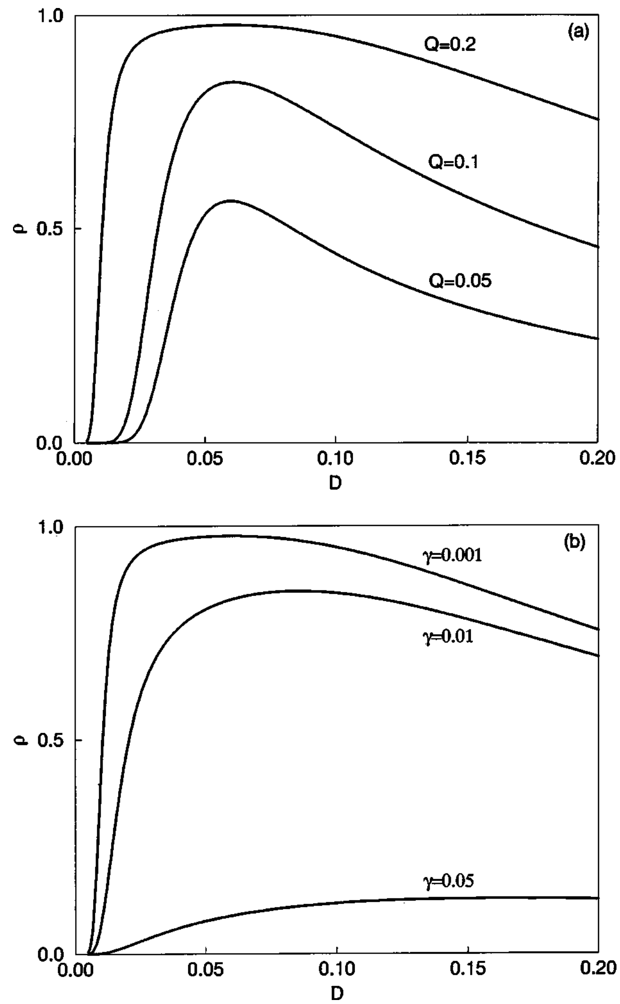

FIG. 2. Correlation coefficient (13) vs noise intensity for indicated values of signal magnitude Q and fixed flipping rate $\gamma=0.001$ (a), and for different values of flipping rate with fixed magnitude $Q=0.2$ (b). Rates a_1 and a_2 are given by Eqs. (4) with $\Delta U=\frac{1}{4}$ and $\alpha_0=1/(\sqrt{2}\pi)$.

Another appropriate measure for synchronization is the coherence function [8,32] obtained from the spectral densities of the two-dimensional process $\{\sigma(t),d(t)\}$:

$$\Gamma^2(\omega)=\frac{|G_{\sigma d}(\omega)|^2}{G_{dd}(\omega)G_{\sigma\sigma}(\omega)}. \tag{14}$$

In Eq. (14), $G_{sd}(\omega)$ is the cross-spectral density, and $G_{dd}(\omega)$ and $G_{ss}(\omega)$ are the spectral densities of the input and output, respectively. The largest possible value of the coherence function, 1, refers to the existence of strong dependence between two processes in a certain frequency region. The calculation of the coherence function is straightforward for both the LRT approach [30] and the master equation approach. It is maximal in a low-frequency domain, corresponding to the low-frequency input signal. Again, the coherence is maximal at an optimal noise level.

B. Synchronization as a mean frequency-locking phenomenon

Although the linear measures discussed above show noise-enhanced growth of coherence between input-output processes, they do not attest that the switching processes at the input and output are synchronized in time. We note that in the classical theory of oscillation [1], synchronization is understood as an instantaneous phase-locking or frequency-locking phenomenon. The situation becomes more complicated in the presence of noise. In this case, a statistical description of synchronization should be used [2,11,33]. The instantaneous phase description will be used in Sec. IV for a flow stochastic bistable system. Here we show theoretically the effect of mean switching frequency-locking.

The output two-state stochastic process can be characterized by the mean durations of the upper state and lower state: $\langle T\rangle_+=\langle T\rangle_-$. The mean ''period'' of switching is therefore $\langle T\rangle_s=\langle T\rangle_+ + \langle T\rangle_-$. In the frequency domain, this quantity corresponds to the mean switching frequency (MSF):

$$\langle \omega\rangle_s=\frac{2\pi}{T_s}=\frac{\pi}{\langle T\rangle_\pm}. \tag{15}$$

In the same way, the MSF can be defined for the input dichotomic noise:

$$\langle \omega\rangle_0=\pi\gamma. \tag{16}$$

The simplified kinetic model introduced in the previous sections allows one to calculate the mean switching rate at the output of the system, and then compare it with that at the input. Contrary to the previous analysis, we now impose an absorption boundary condition at the state $\sigma=1$ and seek the mean time of leaving the state $\sigma=-1$. Initially, we suppose that both states $d=\pm 1$ of the dichotomic stochastic signal are equally populated. The same situation was studied in Refs. [24,23] in connection with the effect of resonant activation.

The evolution of probability to find the system in, say the left potential well $P_{-1}(t)=P_{-1,-1}(t)+P_{-1,+1}(t)$, is described by the equations $(d=\pm 1)$

$$\frac{d}{dt}P_{-1,d}=-[W_{s=-1\to s=1}(d)+\gamma]P_{-1,d}+\gamma P_{-1,-d}, \tag{17}$$

which have to be solved with the initial condition $P_{-1,-1}(t=0)=P_{-1,+1}(t=0)=\frac{1}{2}$. The eigenvalues are

$$r_{1,2}=\frac{1}{2}[a_1+a_2+2\gamma\pm\sqrt{(a_1-a_2)^2+4\gamma^2}]. \tag{18}$$

The global relaxation rate is determined by the smaller eigenvalue, which also give an estimation of the MSF:

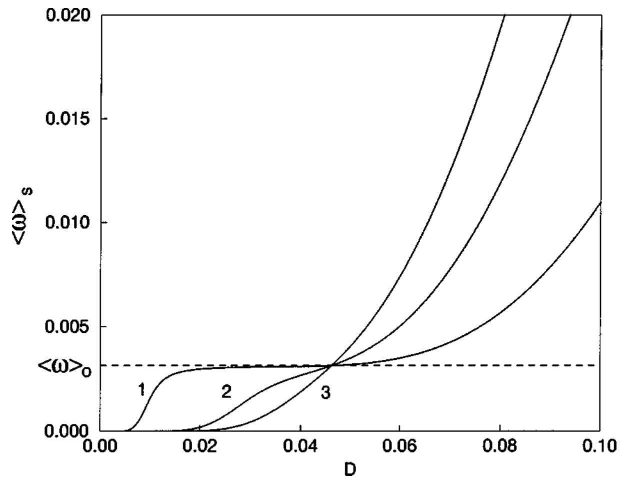

FIG. 3. Mean switching frequency (MSF) vs noise intensity D for different values of signal magnitude: $Q=0.05$ (1), $Q=0.1$ (2), and $Q=0.2$ (3). Other parameters are the same as in Fig. 2. The MSF at the input is shown by the dashed line.

$$\langle \omega\rangle_s=\frac{\pi}{2}[a_1+a_2+2\gamma-\sqrt{(a_1-a_2)^2+4\gamma^2}]. \tag{19}$$

The MSF versus noise intensity is shown in Fig. 3 for different values of the signal magnitude Q. For small Q, the dependence $\langle \omega\rangle_s(D)$ follows the exponential Arrhenius law. However, for larger driving magnitudes, the Arrhenius law breaks down, and for a large enough Q, the MSF is nearly constant over a range of noise intensities and equals the mean switching frequency of the input signal $(\pi\gamma)$. For small noise, $a_2(D)\ll\gamma$ and the MSF approaches $\pi a_1/2$, whereas for large noise, $\langle \omega\rangle_s$ approaches πa_2 [24]. In other words, the MSF is locked in a *finite* region of noise intensity in the same way as it was observed for periodically driven stochastic bistable systems [9,11]. We also note that qualitatively the same mean frequency versus driving frequency behavior can be observed in synchronized limit-cycle oscillators [2]. In our case, we change the noise intensity, which is equivalent to changing the characteristic time-scale of the system. We note that this is the first theoretical evidence of stochastic synchronization as an MSF-locking effect.

Imposing the condition

$$|\langle \omega\rangle_s-\pi\gamma|\leq\epsilon,\quad \epsilon\ll 1, \tag{20}$$

we can obtain a region of MSF locking in the parameter plane of noise intensity versus signal magnitude. These synchronization regions are shown in Fig. 4 for different values of flipping rate. MSF-locking regions look similar to Arnold tongues, and their width decreases with an increase in flipping rate in the same manner as for periodically driven stochastic bistable systems [9]. The tongues occur even for $Q=0$. However, they have a distinguishable width only for sufficiently large input-signal magnitudes (see also Fig. 3).

IV. SYNCHRONIZATION OF AN OVERDAMPED BISTABLE OSCILLATOR BY DICHOTOMIC NOISE

The overdamped bistable oscillator is governed by the stochastic differential equation

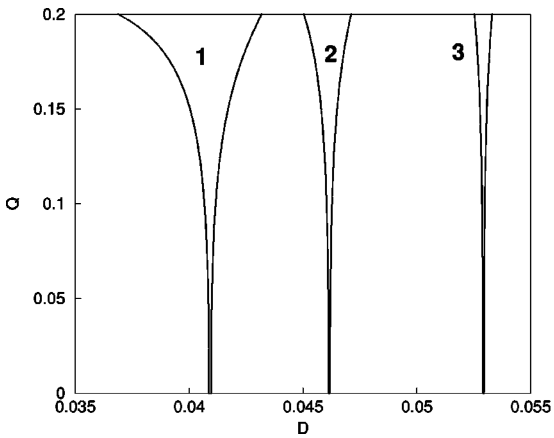

FIG. 4. Regions of MSF-locking defined by Eq. (20) with $\epsilon = 10^{-5}$ for different values of the flipping rate: $\gamma = 0.0005$ (1), $\gamma = 0.001$ (2), and $\gamma = 0.002$ (3).

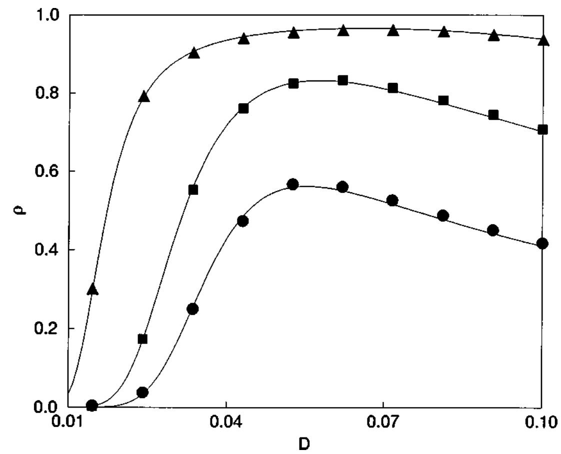

FIG. 5. Correlation coefficient obtained from numerical simulation of Eq. (21) (symbols) and theoretical prediction (13) (solid lines) vs noise intensity for different values of signal magnitude: $Q = 0.05$ (circles), $Q = 0.1$ (squares), and $Q = 0.2$ (triangles). The flipping rate of the signal $\pi\gamma = 0.002$.

$$\dot{x} = x - x^3 + Qd(t) + \sqrt{2D}\xi(t), \tag{21}$$

where $\xi(t)$ is internal (or thermal) noise with intensity D, and $d(t)$ is dichotomic noise with flipping rate γ.

We assume that the magnitude of the dichotomic noise is always small, i.e., the signal alone cannot cause the noise-free system (i.e., a system with no internal noise) to switch from one state to another. For low-frequency modulation, this requires that

$$Q < Q_0 = \frac{2}{3\sqrt{3}}. \tag{22}$$

Recently, similar models, but with multiplicative noise, have attracted considerable attention due to the effect of resonant activation [25]. In addition, aperiodic stochastic resonance in this model was studied in Ref. [34].

In the absence of an external signal ($Q = 0$), the stochastic dynamics of system (21) is characterized by the Kramers time T_K [27] for transitions between potential wells, or by the mean switching frequency, in the frequency domain. This time scale is fully controlled by noise and (in the absence of an external signal) follows Kramers law:

$$T_K = \sqrt{2}\pi \exp\left(\frac{1}{4D}\right). \tag{23}$$

In the following subsections, we present the results of numerical simulations of Eq. (21). To compare these results with the theoretical predictions of the previous sections, we have filtered out intrawell motion, so that the output process represents the two-state dynamics of the system. We take $\langle\omega\rangle_0 = \pi\gamma = 0.002$, which provides good separation of the system time scales.

A. Correlation coefficient

We start with cross-correlation measures. The correlation coefficient is shown in Fig. 5 (symbols) as a function of internal noise intensity for different values of signal magnitude. To compare these numerical results with the theoretical prediction [Eq. (13)], we note that, since the potential profile changes considerably for a signal of large magnitude Q, the Kramers formula (23) is violated. Consequently, we calculate the rates $a_{1,2}$ using the mean first passage time theory [27]: for the overdamped bistable system (21), the rates $a_{1,2}$ can be found through the mean first passage time to the top of the potential barrier in the adiabatic approximation of slowly varying dichotomic noise, i.e., the flipping rate of the noise is much less than the relaxation rates inside the potential wells. We first locate the extrema of the potential $U(x) = -x^2/2 + x^4/4$ from the cubic equation $x^3 - x \pm Q = 0$. We let $x_0^{\pm}$ be the coordinate of the top of the potential, and $x_1^{\pm}$ be the coordinate of the left bottom. For the mean first passage time $T^{\pm}$ to reach the top of the potential, we find [27]

$$T^{\pm} = \frac{1}{D}\int_{x_1^{\pm}}^{x_0^{\pm}} \frac{dy}{G^{\pm}(y)} \int_{-\infty}^{y} G^{\pm}(z)\,dz, \tag{24}$$

$$G^{\pm}(x) = \exp\left[\frac{1}{D}\left(\frac{x^2}{2} - \frac{x^4}{4} \mp Qx\right)\right].$$

Substituting the rates $a_{1,2} = 1/2T^{\mp}$ into Eq. (13), we obtain the correlation coefficient for the overdamped bistable oscillator.

Theoretical curves are shown in Fig. 5 as solid lines, and demonstrate nearly perfect agreement with the numerical results, although intrawell dynamics has been neglected. We underline that in contrast to the previous studies of aperiodic stochastic resonance, our theory is able to cover the strictly nonlinear regime, where the signal magnitude is comparable with the potential barrier. For large-magnitude dichotomic noise, the dependence $\rho(D)$ flattens, and the correlation coefficient remains nearly constant in a finite region of noise intensity. For small signal amplitudes ($Q < 0.01$), LRT can be used. In this case, intrawell dynamics can be taken into account through the calculation of the susceptibility [21,28], which gives nearly the same results for the correlation coefficient as Eq. (13) (differences appear only for very small values of noise intensity).

B. Phase synchronization

Let us now consider the phenomenon of synchronization from the classical viewpoint of phase locking. In this context, we take synchronization to mean that the times t_k at which the dynamical variable $x(t)$ of system (21) switches from one potential well to another are in agreement with the switching times τ_m of the external signal. Thus information about the phase is carried by the switching times t_k, and therefore, the intrawell dynamics of the bistable system are not important for our analysis. We introduce instantaneous phases $\Phi(t)$ and $\Psi(t)$ of the system and signal, respectively, using the ansatz [11]

$$x(t)=x_m\,\mathrm{sgn}[\cos\Phi(t)],\quad d(t)=Q\,\mathrm{sgn}[\cos\Psi(t)], \tag{25}$$

where $\Phi(t)$ and $\Psi(t)$ are defined from the switching times of the system and dichotomic noise, respectively [35]:

$$\Phi(t)=\pi\frac{t-t_k}{t_{k+1}-t_k}+\pi k,\quad t_k<t<t_{k+1},$$
$$\Psi(t)=\pi\frac{t-\tau_m}{\tau_{m+1}-\tau_m}+\pi m,\quad \tau_m<t<\tau_{m+1}, \tag{26}$$

and x_m stands for the half-distance between the bistable attractors. From Eqs. (26), it follows that the phase $\Phi(t)$ is a piecewise linear function that increases by 2π after every round trip from one potential well to another and back again. The mean frequency $\langle\omega\rangle=\langle\partial_t\Phi(t)\rangle$ for such a definition of the phase is

$$\langle\omega\rangle=\lim_{M\to\infty}\frac{1}{M}\sum_{k=1}^{M}\frac{\pi}{t_{k+1}-t_k}. \tag{27}$$

The quantity of interest for our study is the phase difference $\phi(t)=\Phi(t)-\Psi(t)$. The condition for the phase synchronization of the noise-free system is [36]

$$|\phi(t)|<\mathrm{const.} \tag{28}$$

This condition also implies frequency locking between the system and the driving signal. However, for noisy systems, the definition of phase synchronization is not as straightforward because of noise-induced phase diffusion [2]. For instance, for the case of a noisy oscillator synchronized by a harmonic force, the phase difference performs Brownian-like motion in a tilted periodic potential [2]. That is, the phase difference stays for a considerable time in a potential well, which corresponds to the phase-locking segments, and rarely makes jumps between potential wells, demonstrating phase slips. Given these effects, there are several ways to define the notion of synchronization for stochastic systems, imposing restrictions on the different functionals of the systems [11,20]. In particular, here we impose the following restriction on the fluctuations of the phase difference: the mean duration of the phase-locking segments must be large in comparison with the characteristic time scale of the driving signal.

Synchronization of stochastic systems can also be evidenced by the mean frequency-locking effect. We calculated the MSF equation (27) of system (21) as a function of the internal noise intensity for different values of the driving-signal amplitude—see Fig. 6. This figure shows the effect of MSF locking. We also note good agreement between the theory [Eq. (19)] and numerical simulations.

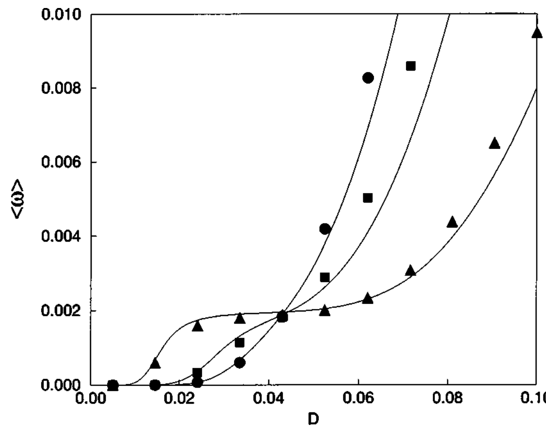

FIG. 6. Mean frequency $\langle\omega\rangle$ of the overdamped bistable oscillator vs internal noise intensity D for different values of the magnitude Q of the external dichotomic noise: $Q=0.05$ (circles), $Q=0.1$ (squares), and $Q=0.2$ (triangles). The flipping rate of the signal $\pi\gamma=0.002$. The theoretical curves for the MSF $\langle\omega\rangle_s$ from Eq. (19), with rates a_1 and a_2 calculated from Eq. (24), are shown as solid lines.

Figure 7 shows the time series for the phase difference $\phi(t)$ for different levels of internal noise. The evolution of $\phi(t)$ is similar to that of classically synchronized oscillators with noise: there are patterns of nearly constant phase difference (referring to the phase-locked regimes), interrupted by phase slips (the phase difference makes jumps of 2π). In Fig. 7, the duration of the phase-locked segments is maximized at a particular noise intensity. For weak noise, the MSF is smaller than the flipping rate of the dichotomic noise and the phase of the dichotomic noise surpasses the phase of the system. In contrast, for large noise intensities, the phase of the driving signal lags the system phase and the MSF becomes larger than the flipping rate.

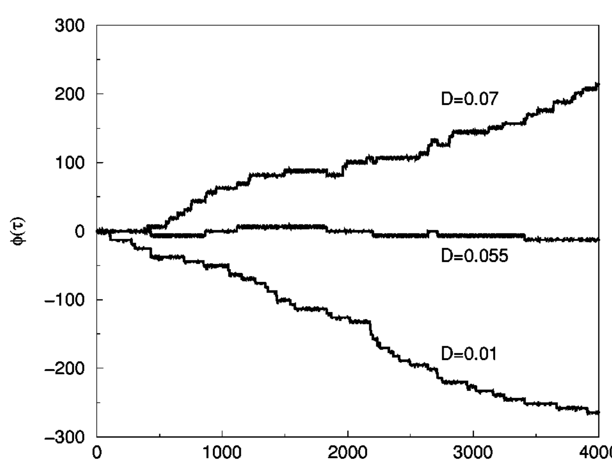

FIG. 7. Instantaneous phase difference $\phi(\tau)$ for the overdamped bistable oscillator for indicated values of the internal noise intensity D, with $Q=0.3$, $\pi\gamma=0.002$. The time axis is given in the units of the mean switching frequency of dichotomic noise: $\tau=t\pi\gamma$.

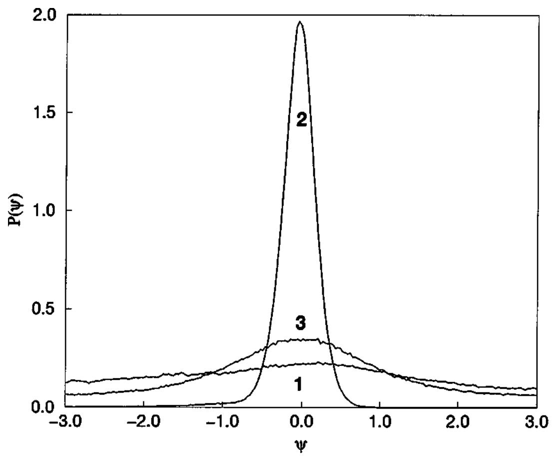

FIG. 8. Probability density of the wrapped phase difference for different values of noise intensity: $D=0.01$ (1), $D=0.044$ (2), and $D=0.2$ (3). Other parameters are $Q=0.2$ and $\pi\gamma=0.002$.

This noise-enhanced phase coherence becomes more evident if we calculate the probability density of the phase difference ψ wrapped up in the $[-\pi,\pi]$ region: $\psi=\phi(t) \bmod 2\pi$. We show the probability densities $P(\psi)$ of the wrapped phase difference for different noise intensities in Fig. 8. At an optimal noise intensity, $P(\psi)$ possesses a well-expressed narrow peak: the width of the distribution is minimal, while its height is maximal. For very weak or very large noise, the probability density of the phase difference becomes nearly uniform.

To quantify this behavior, we can use the ratio of the distribution height, $P_{\max}$, to the variance of the phase difference as a measure of the phase coherence:

$$R=P_{\max}\left\{\int_{-\pi}^{\pi}\psi^2 P(\psi)d\psi-\left[\int_{-\pi}^{\pi}\psi P(\psi)d\psi\right]^2\right\}^{-1/2}. \tag{29}$$

In our situation, the quantity R can be considered as an equivalent of the signal-to-noise ratio. Both the variance of the wrapped phase and the height of the probability distribution pass through extrema when plotted against D: the variance possesses a minimum, while the $P_{\max}$ has a maximum. As the result, the ratio R passes through a single maximum, indicating noise-enhanced growth of the phase coherence. The phase coherence measure R is shown in Fig. 9 as a function of noise intensity for different values of the signal magnitude Q.

Finally, we calculate the effective diffusion constant defined as

$$D_{\mathrm{eff}}=\frac{1}{2}\frac{d}{dt}[\langle\phi^2(t)\rangle-\langle\phi(t)\rangle^2], \tag{30}$$

which describes the spreading of an initial distribution of the phase difference. The noise-enhanced phase coherence [11] is manifested through the existence of a minimum in the dependence of D_{eff} on D (see Fig. 10): for a large enough magnitude of dichotomic noise, the effective diffusion constant can be minimized, which corresponds to longer phase-locking epochs [2] (see Fig. 7).

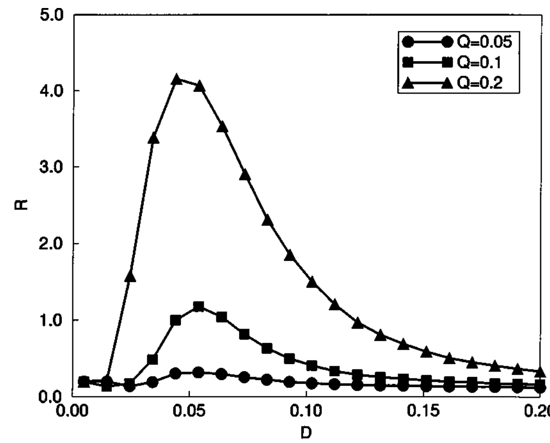

FIG. 9. Ratio (29) vs noise intensity for indicated values of signal magnitude. Other parameters are the same as in Fig. 8.

V. SYNCHRONIZATION OF A STOCHASTIC NEURON MODEL BY A STOCHASTIC SPIKE TRAIN

Similar effects can be observed in stochastic neuron models. In such cases, it is more interesting and appropriate to consider a stochastic spike train rather than dichotomic noise as the external stochastic driving signal. We can think about a single neuron embedded in a neuronal network with the stochastic spike train representing the summed output of all the neurons in the network that are directly coupled to the neuron of interest. We use stochastic sequences of impulses as the model for the stochastic spike train.

We study an integrate-and-fire (IF) model neuron with inhibitory synaptic feedback that is driven by internal white noise and an external stochastic impulse train [37]. The model is governed by the following stochastic differential equations

$$\dot{v}=-\frac{v}{\alpha}+I_0+Q\nu(t)-kw+\sqrt{2D}\xi(t),$$
$$\dot{w}=-\Gamma w+\sum_{i=0}^{\infty}\delta(t-t_i), \tag{31}$$

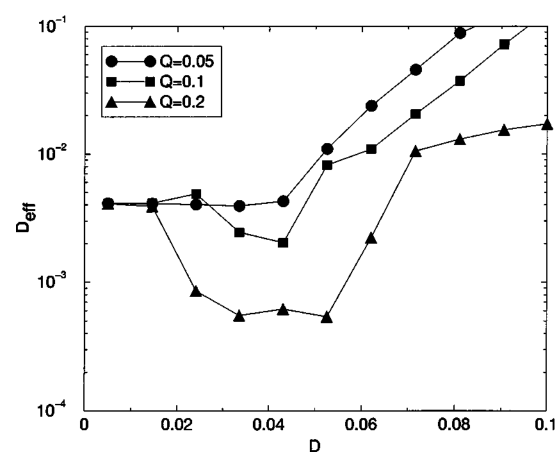

FIG. 10. The effective diffusion constant (30) vs noise intensity for indicated values of signal magnitude. Other parameters are the same as in Fig. 9.

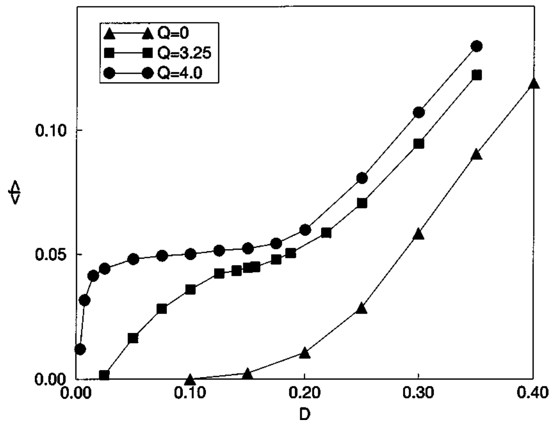

FIG. 11. Mean firing rate for the integrate-and-fire model neuron (31) $\langle f \rangle$ vs internal noise intensity D for the indicated values of the magnitude Q of the external stochastic pulse train. Parameters: $\alpha=0.1$, $I_0=5$, $k=10^3$, $\Gamma=0.8$, $\gamma=0.05$, and $\tau_s=\gamma^{-1}/10$.

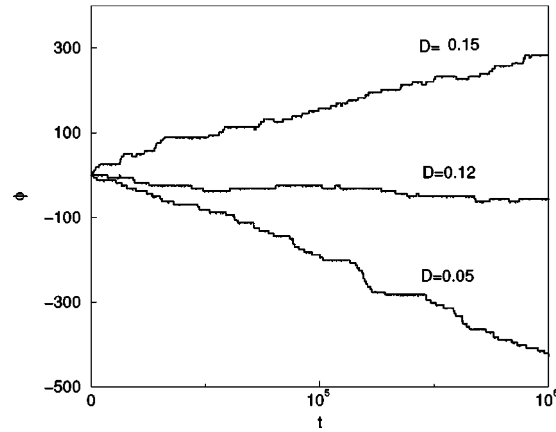

FIG. 12. Instantaneous phase difference $\phi(t)$ for the integrate-and-fire model neuron (31) for different values of the internal noise intensity D and $Q=4$. Other parameters are the same as in Fig. 11.

where α is the membrane time, I_0 is a constant current term, Γ is the inverse synaptic time, t_i are the moments in time when the neuron fires, $\xi(t)$ is the internal white noise, and $\nu(t)$ is the external stochastic pulse train. The variable v is reset to $v=0$ every time it reaches the threshold $v=1$. Pulses appear at random times τ_n with exponentially distributed intervals between pulses $\Delta\tau$, $P(\Delta\tau)=\gamma e^{-\gamma\Delta\tau}$, and the time duration of each pulse is equal to $\tau_s \ll 1/\gamma$. We consider only the subthreshold regime, so that there are no spikes in the variable $v(t)$ in the absence of the internal noise ($D=0$). Numerical results for the mean firing rate for the IF model neuron are shown in Fig. 11. It can be seen that there is a region of noise intensity where the mean firing rate of the model neuron is locked by the external stochastic signal for large enough Q. The differences between the frequency-locking curves of Fig. 11 and those for the overdamped bistable oscillator appear to be due to the asymmetry of the IF model and the imposed stochastic spike train.

The instantaneous phase of system (31) can be reasonably defined using the firing times t_k. The phases $\Phi(t)$ and $\Psi(t)$ of the system and stochastic spike train, respectively, are given by

$$\Phi(t)=2\pi\frac{t-t_k}{t_{k+1}-t_k}+2\pi k, \quad t_k<t<t_{k+1},$$
$$\Psi(t)=2\pi\frac{t-\tau_m}{\tau_{m+1}-\tau_m}+2\pi m, \quad \tau_m<t<\tau_{m+1}, \tag{32}$$

so that the phases are changed by 2π with each firing event. The mean frequencies of the system and stochastic spike train, respectively, are simply their mean firing rates. Our numerical results for the IF model neuron (Fig. 12) again display the effect of phase synchronization.

VI. SUMMARY

This work shows that the synchronization of noisy systems by stochastic signals manifests itself through instantaneous phase-locking and mean frequency locking, as well as through the growth of coherence measures. In real-world applications, it is common for both the system and driving signal to be noisy. In this study, we considered stochastic systems that ''oscillate'' because of internal noise. We found that the temporal behavior of such systems can be synchronized by external stochastic signals. This result may be relevant to problems in neurobiology, such as precision timing of neurons [16], given that neurons and their inputs are typically noisy.

ACKNOWLEDGMENTS

We thank C.C. Chow, J. Freund, and P. Jung for fruitful discussions. This work was supported by the Fetzer Institute, the U.S. Office of Naval Research, the U.S. Department of Energy, the National Science Foundation, and by DFG, SFB 555.

[1] A. Andronov, A. Vitt, and S. Khaykin, *Theory of Oscillations* (Pergamon Press, Oxford, 1966); C. Hayashi, *Nonlinear Oscillations in Physical Systems* (McGraw-Hill, New York, 1964); I. Blekhman, *Synchronization of Dynamical Systems* (Nauka, Moscow, 1971) (in Russian); I. Blekhman, *Synchronization in Science and Technology* (Nauka, Moscow, 1981; English translation: ASME Press, New York, 1988).

[2] R. L. Stratonovich, *Topics in the Theory of Random Noise* (Gordon and Breach, New York, 1967), Vol. 2.

[3] V. S. Afraimovich, N. N. Verichev, and M. I. Rabinovich, Radiophys. Quantum Electron. **29**, 795 (1986).

[4] L. Pecora and T. Carroll, Phys. Rev. Lett. **64**, 821 (1990).

[5] M. Rosenblum, A. Pikovsky, and J. Kurths, Phys. Rev. Lett. **76**, 1804 (1996).

[6] N. F. Rulkov, K. M. Sushchik, L. S. Tsimring, and H. D. I. Abarbanel, Phys. Rev. E **51**, 980 (1995).

[7] L. Kocarev and U. Partlitz, Phys. Rev. Lett. **74**, 5028 (1995).

[8] A. Neiman, Phys. Rev. E **49**, 3484 (1994).

[9] B. Shulgin, A. Neiman, and V. Anishchenko, Phys. Rev. Lett. **75**, 4157 (1995).

[10] A. Longtin, Nuovo Cimento D **17**, 835 (1995); Chaos **5**, 209 (1995); A. Longtin and D. R. Chialvo, Phys. Rev. Lett. **81**, 4012 (1998).

[11] A. Neiman, A. Silchenko, V. Anishchenko, and L. Schimansky-Geier, Phys. Rev. E **58**, 7118 (1998).

[12] A. Silchenko, T. Kapitaniak, and V. Anishchenko, Phys. Rev. E **59**, 1593 (1999).

[13] J. J. Collins, C. C. Chow, and T.T. Imhoff, Phys. Rev. E **52**, R3321 (1995); Nature (London) **376**, 236 (1995); J. J. Collins, T. T. Imhoff, and P. Grigg, J. Neurophysiol. **76**, 642 (1996); C. Heneghan, C. C. Chow, J. J. Collins, T. T. Imhoff, S. B. Lowen, and M. C. Teich, Phys. Rev. E **54**, R2228 (1996); J. J. Collins, C. C. Chow, A. C. Capela, and T. T. Imhoff, Phys. Rev. E **54**, 5575 (1996); P. C. Gailey, A. Neiman, J. J. Collins, and F. Moss, Phys. Rev. Lett. **79**, 4701 (1997); C. C. Chow, T. T. Imhoff, and J. J. Collins, Chaos **8**, 616 (1998).

[14] L. J. DeFelice, *Introduction to Membrane Noise* (Plenum, New York, 1981); R. D. Astumian and B. Robertson, J. Chem. Phys. **91**, 4891 (1991); A. Fuliński, Phys. Rev. Lett. **79**, 4926 (1997).

[15] M. M. Millonas and D. A. Hanck, Phys. Rev. Lett. **80**, 401 (1998).

[16] Z. F. Mainen and T. J. Sejnowski, Science **268**, 1503 (1995); X. Pei, L. Wilkens, and F. Moss, Phys. Rev. Lett. **77**, 4679 (1996).

[17] R. Benzi, A. Sutera, and A. Vulpiani, J. Phys. A **14**, L453 (1981); R. Benzi, G. Parisi, A. Sutera, and A. Vulpiani, Tellus **34**, 10 (1982); C. Nicolis, *ibid.* **34**, 1 (1982).

[18] See, for reviews, F. Moss, in *Some Contemporary Problems in Statistical Physics*, edited by G. Weiss (SIAM, Philadelphia, 1994), p. 205; F. Moss, D. Pierson, and D. O'Gorman, Int. J. Bifurcation Chaos Appl. Sci. Eng. **4**, 1383 (1994); K. Wiesenfeld and F. Moss, Nature (London) **373**, 33 (1995); A. R. Bulsara and L. Gammaitoni, Phys. Today **49** (3), 39 (1996).

[19] L. Gammaitoni, P. Hänggi, P. Jung, and F. Marchesoni, Rev. Mod. Phys. **70**, 223 (1998).

[20] V.S. Anishchenko, A. Neiman, F. Moss, and L. Schimansky-Geier, Usp. Fiz. Nauk **169**, 7 (1999) [Sov. Phys. Usp. **42**, 7 (1999)].

[21] M. I. Dykman, R. Mannella, P. V. E. McClintock, and N. G. Stocks, Phys. Rev. Lett. **65**, 2606 (1990); M. I. Dykman, R. Mannella, P. V. E. McClintock, and N. G. Stocks, Pis'ma Zh. Éksp. Teor. Fiz. **52**, 780 (1990) [JETP Lett. **52**, 144 (1990)] P. Jung and P. Hänggi, Phys. Rev. A **44**, 8032 (1991); D. G. Luchinsky, P. V. E. McClintock, and M. I. Dykman, Rep. Prog. Phys. **61**, 889 (1998).

[22] P. Debye, *Polar Molecules* (Dover, New York, 1929).

[23] C. Van den Broeck, Phys. Rev. E **47**, 4579 (1993).

[24] U. Zücher and C. R. Doering, Phys. Rev. E **47**, 3862 (1993).

[25] C. R. Doering and J. C. Gadoua, Phys. Rev. Lett. **69**, 2318 (1992); P. Pechukas and P. Hänggi, *ibid.* **73**, 2772 (1994); P. Reimann and T. C. Elston, *ibid.* **77**, 5328 (1996); M. Boguna, J. M. Porrà, J. Mausoliver, and K. Lindenberg, Phys. Rev. E **7**, 3990 (1998); P. Reimann and P. Hänggi, in *Stochastic Dynamics*, edited by L. Schimansky-Geier and T. Pöschel (Springer, Berlin, 1997), pp. 127–139.

[26] B. McNamara and K. Wiesenfeld, Phys. Rev. A **39**, 4854 (1989).

[27] P. Hänggi, P. Talkner, and M. Borkovec, Rev. Mod. Phys. **62**, 251 (1990).

[28] P. Jung, Phys. Rep. **234**, 175 (1995).

[29] M. I. Dykman, D. G. Luchinsky, R. Mannella, P. V. E. McClintock, N. D. Stein, and N. G. Stocks, Nuovo Cimento D **17**, 661 (1995).

[30] A. Neiman, L. Schimansky-Geier, and F. Moss, Phys. Rev. E **56**, R9 (1997).

[31] M. H. Choi, R. F. Fox, and P. Jung, Phys. Rev. E **58**, 6335 (1998); F. Marchesoni, F. Apostolico, and S. Santucci, Phys. Lett. A **248**, 332 (1998).

[32] A. Neiman and L. Schimansky-Geier, Phys. Lett. A **197**, 379 (1995).

[33] P. Tass, M. G. Rosenblum, J. Weule, J. Kurths, A. Pikovsky, J. Volkman, A. Schnitzer, and H.-J. Freund, Phys. Rev. Lett. **81**, 3291 (1998).

[34] X. Godivier and F. Chapeau-Blondeau, Int. J. Bifurcation Chaos Appl. Sci. Eng. **8**, 581 (1998).

[35] The same definition for the phase of chaotic systems has been used in A. Pikovsky, M. Rosenblum, G. Osipov, and J. Kurths, Physica D **104**, 219 (1997); M. Rosenblum, A. Pikovsky, and J. Kurths, IEEE Trans. Circuits Syst. **44**, 874 (1997).

[36] E. Ott, *Chaos in Dynamical Systems* (Cambridge University Press, Cambridge, 1992).

[37] C. C. Chow, Physica D **118**, 343 (1998); D. J. Mar, C. C. Chow, W. Gerstner, R. W. Adams, and J. J. Collins (unpublished).